HEFAT2010
7th International Conference on Heat Transfer, Fluid Mechanics and Thermodynamics
19-21 July 2010
Antalya, Turkey

EFFECT OF THE DAYS SCROLLING ON THE NATURAL CONVECTION IN AN OPEN ENDED STORAGE SILO

Ameziani D.E.[1,2], Bouhadef K.[1*], Bennacer R.[2]
*Author for correspondence
[1] Laboratoire LTPMP, Faculté de Génie Mécanique et Génie des Procédés
USTHB University
B.P.32 , El Alia, Bab Ezzouar, 16111. ALGIERS
ALGERIA.
[2] Laboratoire LEEVAM
Cergy Pontoise university
5 mail Gay Lussac 95031, Neuville sur Oise
FRANCE.

ABSTRACT

The problem of unsteady natural convection heat transfer in a vertical open ended porous cylinder heated with a sinusoidal time variation of the lateral wall temperature has been investigated numerically The used flow model is the classical Darcy model. In the case of constant wall temperature two types of flows, with and without fluid recirculation, depending on the filtration Rayleigh (*Ra*), the aspect ratio (*A*) and the inlet-outlet conditions (*Bi*) have been obtained. For the low dimensionless amplitudes case ($XA<0.5$), a large equivalence in the heat transfer between the sinusoidal time variation and the constant wall temperature is demonstrated with a difference is less than 5%. For high Ra, the difference increases.

INTRODUCTION

Several devices are transiently provided by energy such as the solar energy collectors, circuits' alimented by alternating current, storage in ambient conditions, etc. Therefore, the knowledge of the mechanisms of heat transfer by transient convection becomes necessary, especially as it is difficult to predict the behaviour of a fluid submitted to variable conditions of heating, from results obtained with conditions of temperatures or fluxes imposed constant.

Many papers dealt with constant time-variation of temperature or flux in fluids (Patterson and Imberger [1], Vasseur and Robillar [2]). In the case of periodical heating conditions, Kazmierezak and Chinoda [3] were interested to the transient natural convection in a square cavity, due to a periodical variation of the temperature of the hot vertical wall. The opposite wall was maintained cold. All the obtained transients' solutions were periodic on time and showed that in spite of the dependence of the boundary conditions on time and the variations of the dynamical and thermal fields, the average heat transfer evaluated on one temporal cycle, was roughly equal to the value obtained when the hot wall was at constant temperature.

Time-dependent heating in porous medium has been the subject of relatively few previous studies. Thus, Sözen and Vafai [4] analyzed compressible flow through a packed bed with the inlet temperature or pressure oscillating with time about a nonzero mean. They found that the oscillation had little effect on the heat storage capacity of the bed. Bradean *et al.* ([5], [6]) gave an analytical and numerical treatment for a periodically heated and cooled vertical or horizontal plate. They found that for the vertical plate, a row of counter-rotating cells formed close to the surface, but when the Rayleigh number increased above 40, the cellular flow is separated from the plate. For the horizontal plate, the separation did not occur.

The aim of the present work is to treat numerically the problem of unsteady natural convection which occurs in a vertical silo of granular storage, opened at both ends. The lateral wall is maintained at a sinusoidal temperature to simulate the scrolling of the days and the years (by changing the period).

MATHEMATICAL FORMULATION

The problem under consideration (natural convection in open geometry) seems to be of a particularly delicate numerical resolution. Indeed, the flow rate of the fluid in the channel is fixed only indirectly by the intensity of the heated wall. Consequently, most of the authors do not apply the same boundary conditions for the resolution of the problem. An illustration of the inaccuracy, the recent established benchmark problem of chimney effect was discussed by Desrayaud *et al.* ([7]. The difference remains also for the same problem with different boundary conditions and a flow reversal in the channel exit is obtained by several authors (Krishnan [8], Hernandez and Zamora [9]).

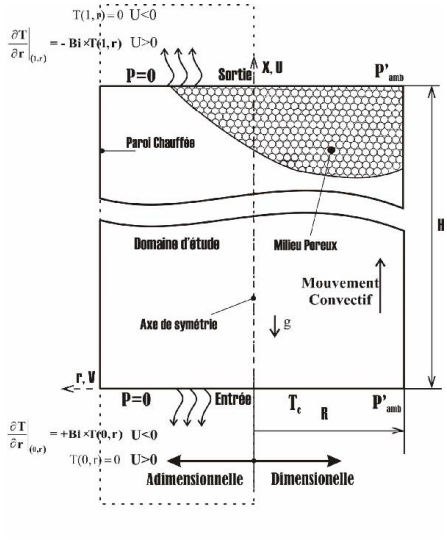

Figure 1 Geometrical configuration.

The physical domain of the flow through the vertical porous cylinder is given in Figure 1. It is assumed that the flow in the cylinder is axis-symmetric allowing a two-dimensional approach. The porous medium is considered to be homogeneous, isotropic and saturated with a pure single phase fluid, which is in thermal equilibrium with the solid matrix. The fluid thermo-physical properties are assumed to be constant, except in the body force term of the momentum equations invoking the Boussinesq's approximation. The current study assumes the validity of the Darcy flow model.

The analysis is performed in terms of non-dimensional parameters that successfully cast together all the pertinent influencing effects. To this end, the non dimensionalization of the governing equations and boundary conditions at a macroscopic scale are carried out on the basis of the following references:

$$L_{ref} = H \;;\; \Delta T_{ref} = T'_h - T'_c \;;\; P_{ref} = \left(\mu \cdot \alpha_f / K\right) \;;\; U_{ref} = \alpha_f / H$$

and $t_{ref} = H^2 / \alpha_f$ (1)

The non-dimensional quantities are:

$$(x,r) = (x',r')/L_{ref} \;;\; (U,V) = (U',V')/U_{ref} \;;\; T = \left(T - T_c\right)/\Delta T_{ref} \;;$$

$$P = \left(P' - P'_{amb}\right)/P_{ref} \;;\; t = t'/t_{ref} \quad (2)$$

The resulting dimensionless continuity and the energy equations are as follows:

$$\left(\frac{\partial^2 P}{\partial x^2} + \frac{1}{r}\frac{\partial}{\partial r}\left(r\frac{\partial P}{\partial r}\right)\right) = Ra \cdot \frac{\partial T}{\partial x} \quad (3)$$

$$\sigma\frac{\partial T}{\partial t} + \left(U\frac{\partial T}{\partial x} + V\frac{\partial T}{\partial r}\right) = R_k \cdot \left(\frac{\partial^2 T}{\partial x^2} + \frac{1}{r}\frac{\partial}{\partial r}\left(r\frac{\partial T}{\partial r}\right)\right) \quad (4)$$

The velocity components are deduced from the obtained pressure field:

$$U = Ra \cdot T - \frac{\partial P}{\partial x} \;;\; V = -\frac{\partial P}{\partial r} \quad (5a,b)$$

where Ra is the filtration Rayleigh number ($Ra = g\beta\Delta T_{ref} K H/\left(\nu \cdot \alpha_f\right)$, also called Rayleigh-Darcy number), R_k and σ are respectively the conductivity and calorific capacity ratios (between effective and fluid values).

The dimensionless initial and boundary conditions become:

at t ≤0, it is assumed that the pressure and temperature in the cylinder are considered uniform and equal to the ambient conditions:

$$P(x,r,0) = T(x,r,0) = 0 \quad (6)$$

at t >0, the inlet and outlet fluid are at the ambient pressure, P'_{amb} :

$$P(0,r,t) = P(1,r,t) = 0 \quad (7a,b)$$

Owing to the symmetry requirement at the centreline ($r = 0$) and the impermeable lateral surface of the cylinder, it follows that:

$$\partial P/\partial r\big|_{(x,0,t)} = \partial P/\partial r\big|_{(x,A,t)} = 0 \quad (8a,b)$$

$$\partial T/\partial r\big|_{(x,0,t)} = 0 \quad (9)$$

The raison which enlightens this study is the problem of the high ambient temperature fluctuations in some regions. Many authors give the ambient temperature as a sum of sinusoidal functions (Boland [10] for the region of Laverton in Australia).

The lateral wall temperature is supposed at the ambient one and can be approached by a sinusoidal time-variation (Figure. 2):

$$T(x,A,t) = 1 + XA \cdot \sin\left(\left(2\pi/\tau\right) \cdot t\right) \quad (10)$$

where A is the cylinder aspect ratio A=R/H, XA and τ are respectively the dimensionless oscillation amplitude ($a/\Delta T_{ref}$, where $a = \left(T_{Max} - T_{Min}\right)/2$), and the period of the sinusoidal variation of wall temperature.

The period can simulate both the scrolling of the days or the years ($\tau_{day}=\tau_{year}/365$). The amplitude gives the maximum variation of the temperature which depends on the geographical situation. To consider the general physical conditions at the bottom and upper surfaces, expressing the interaction between the natural convection through the porous media surfaces and the external ambient fluid, we use:

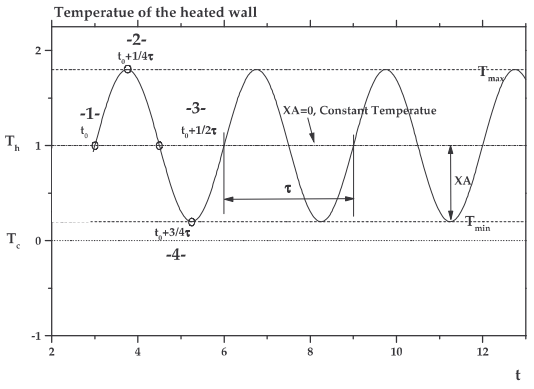

Figure 2 Time evolution of the heated wall temperature

For top surface:

if U>0 (outgoing flow) $\partial T/\partial x\big|_{(1,r,t)} = -Bi \times T(1,r,t)$ (11-a)

if U<0 (ingoing flow) $T(1,r,t) = 0$ (11-b)

For bottom surface:

if U>0 (ingoing flow) $T(0,r,t) = 0$ (12-a)

if U<0 (outgoing flow) $\partial T/\partial x\big|_{(0,r,t)} = +Bi \times T(0,r,t)$ (12-b)

where $Bi = h \cdot H/k_{eff}$ represents the equivalent Biot number of the porous matrix-air interface. h is the convective exchange coefficient and k_{eff} the porous media effective conductivity.

Heat transfer is represented in term of local Nusselt number defined as:

$$Nu(x,t) = -\partial T(x,r,t)/\partial r\big|_{r=A} \quad (13)$$

The space averaged Nusselt number along the cylinder:

$$Nu = Nu(t) = \overline{Nu}(x,t) = \int_0^1 Nu(x,t)\cdot dx \quad (14)$$

And the time-averaged total Nusselt number:

$$Nu_T = \frac{1}{\tau}\int_0^{\tau} Nu(t)\cdot dt \quad (15)$$

The chimney effect and the resulting transient dimensionless total flow rate is expressed as:

$$Q_T(t) = 2\pi \int_0^A U(1,r,t)\cdot r \cdot dr \quad (16)$$

NUMERICAL PROCEDURE

The governing equations (Eqs. 3-5) with the associated initial and boundary conditions (Eqs. 6-12) are solved using the finite volumes method, introduced by Spalding (see Patankar [11]). The resulting algebraic system could be solved by an iterative procedure using the alternate direction implicit method (ADI). The numerical program is tested for both the pure conduction and the classical Darcy natural convection problem in a square porous cavity.

We underline the existence of singularities at the cylinder wall corners, where the cold and hot surfaces are in direct contact, *i.e.*, the local temperature gradient tends to infinity. In physical situation, the relaxation phenomenon induces a connection domain on which the temperature decreases from hot to cold values. To reach the grid independence and convergence to unique solution, essentially for the cases of low Rayleigh numbers, the singularity is treated using temperature regularization on the wall as (see for instance Bennacer *et al.* [12]):

$$f(x) = T(x,A,t) = \left(1-(1-2\cdot x)^{2n}\right)^2 + XA\cdot\sin((2\pi/\tau)\cdot t) \quad (17)$$

The 'n' value controls the domain affected by the temperature transition. It is found that n=50 is enough to reach an asymptotic situation, where no grid effect and only a small domain is affected by the temperature transition (Δx less than 0.001).

In the case of the steady state pure conduction and for a constant applied temperature, the analytical solution is obtained using variable separation and expressed as:

$$T(r,x) = \sum_{m=1}^{m=\infty} [E_{2n}(m)\cdot I_0(\lambda_m \cdot r)\cdot \sin(\lambda_m \cdot x)] \quad (18)$$

where I_0 is the zero order Bessel function , λ_m the solutions of the equation $-\lambda_m = Bi\ tg(\lambda_m)$ and E(m) is the integration coefficients taking into account the external applied irregular temperature condition.

Equation (18) combined with the Nusselt expression (Eq. 14) gives the analytical expression of the resulting heat transfer (averaged Nusselt number) as:

$$Nu = \sum_{m=1}^{m=\infty} [E_{2n}(m)\cdot I_1(\lambda_m \cdot A)\cdot(1-\cos(\lambda_m))] \quad (19)$$

where I_1 is the first order Bessel function.

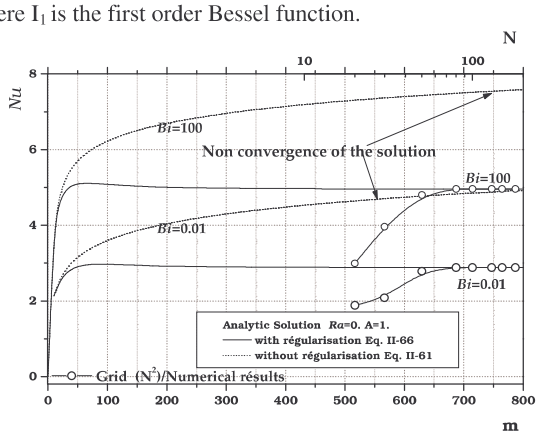

Figure 3 Effect of the regularisation on the analytical solution

The obtained series form solution ('m' in Eq. 19) is represented in Fig. 3. The effect of m values on the corresponding *Nu* with and without regularization (f(x)=1) are compared. We can observe the convergence of the analytical solution with m in case of regularization. The case with singularities at the corners (without regularization $f(x) = T(x,A) = 1$) leads to an obvious non convergence of the obtained analytical solution (Eq. 19). The numerical resolution in such last case can exhibit a relative convergence with grids refinement and induce to an inaccurate conclusion. Details of the validation can be seen in the work of Ameziani *et al.* [13]

RESULTS

The results are presented and discussed in terms of velocity, pressure and temperature fields. Plots showing the evolution of the space and time averaged Nusselt numbers are also presented. Due to the numerous controlling parameters, all the calculations have been performed for a conductivity ratio, aspect ratio and calorific capacity ratio of unity R_k=A=σ=1.

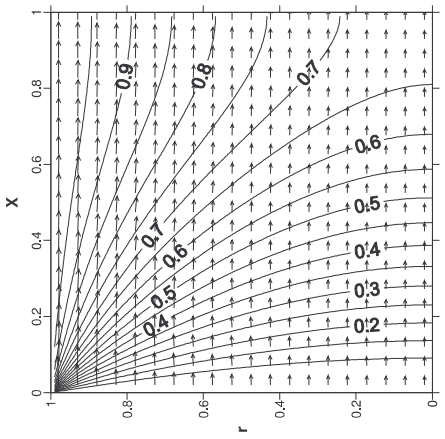

(a)Ra=1, V_{max}=1.44

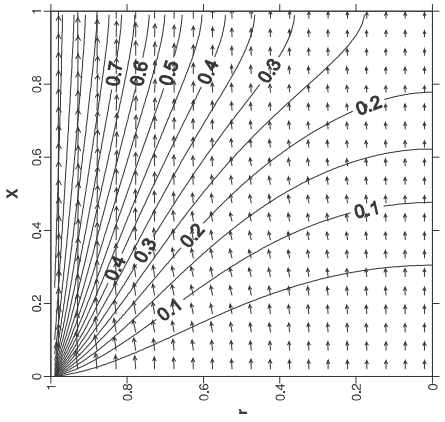

(b)Ra=50, V_{max}=62.33

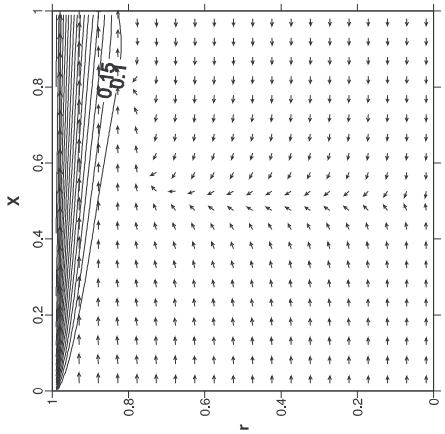

(c)Ra=10^3 V_{max}=1.1334×10^3

Figure 4 Temperature lines and velocity vector field for different *Ra* (*Bi* =0.01, *A*=1, *XA*=0).

Constant wall temperature:

Figure 4 illustrates temperature and velocity fields for different Rayleigh-Darcy numbers in the case of *Bi*=0.01. The isotherms show a similarity with the case of a vertical heated flat plane in a semi-infinite porous medium. The isotherms indicate that the temperature is propagated from the heated vertical cylinder towards the top of the cylinder, creating significant thermal gradients in the horizontal/vertical direction. The flow intensity decreases from the heated wall region to the centre, where thermal buoyancy forces are weak.

The velocity vector field shows that for small filtration Rayleigh number values (*Ra* =1 and 50), the weak flow is ascendant on the entire domain. The fluid flow is mainly unidirectional. When *Ra* increases, the thermal boundary layer is tightened, generating a reduction of thermal gradients in the core of the porous cylinder. In such situation, the velocity values near the wall increase, and the fluid flow in the cylinder is supplied both from the bottom and partially from the top surface of the porous cylinder. This can be explained by the fact that a pressure gradient occurs on the cylinder centre line without buoyancy forces. The resulting volume forces induce a counter-flow in the centreline domain. Such phenomena are the direct consequence of the *Ra* increases, *i.e.* the thermal boundary layer reaches an adequate scale in comparison to the cylinder radius. The reverse flow is observed in both situations of low and high Bi values and the needed Ra condition to obtain such a reverse flow is highly dependent with Bi value and the aspect ratio.

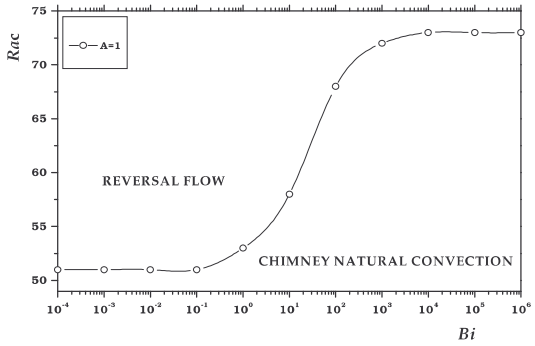

Figure 5 Critical Rayleigh number versus the Biot number for A=1, XA=0.

In the case of aspect ratio, *A*=1, Fig. 5 gives the critical Rayleigh number for the appearance of the top fluid aspiration depending on the different *Bi* values. We can categorize the critical *Ra* behavior into three principal regimes; weak, high and moderate Biot values.

The two first behaviors (weak and high *Bi* values) are a direct consequence of the two extreme situations, (*i.e.* independence of the thermal field with the Biot number) isotherm (*Bi*>>1) or adiabatic (*Bi*<<1) applied boundary conditions. The increase of Ra_c with *Bi* is an effect of the flow intensity (chimney effect) reduction due to the modification of the thermal boundary condition inducing a fluid cooling in the upper cylinder part.

Note that the weak and high *Bi* values exhibit two asymptotic tendency where the needed critical Rayleigh number was respectively Ra_c=52 and 73.

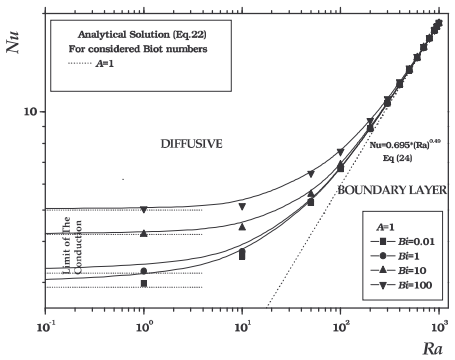

Figure 6 The average Nusselt number versus Ra for different Biot number for A=1, XA=0.

First, the space averaged Nusselt number (Nu_m), for steady constant wall temperature (XA=0) is exhibited in the figure 6 versus Rayleigh and Biot numbers. This plot clearly indicates the increasing of heat transfer with Rayleigh number. The flow enhancement with the buoyancy force increases thermal gradients near the lateral heated wall.

For low Rayleigh values, the heat transfer exhibits asymptotic value corresponding to the diffusive regime. The obtained conductive (low Ra) values are Bi dependent. The analytical conductive heat transfer coefficients (Eq. 19) are plotted for the different analyzed Bi. A good agreement has been obtained and the two dependencies are well estimated.

Note that the heat transfer increases with the Biot number only for low Rayleigh values and this dependence vanishes for high Rayleigh numbers. In such situation (high Ra), the flow tends to a boundary layer structure where the weight effect of the exit boundary condition on the global flow decreases. Consequently all the curves for different Biot numbers go up to a similar limit of the convective mode heat transfer. Such heat transfer variation ($Nu \sim 1/\delta$) is predicted as:

$$Nu \sim \mathrm{Ra}^{1/2} \qquad (20)$$

The Nusselt number in the boundary layer situation is represented by the dashed line on figure 6. The fitted Nu is given by:

$$Nu = 0.695 \times \mathrm{Ra}^{0.49} \qquad (21)$$

Sinusoidal wall temperature:

Figure 7 (a, b) illustrates the temporal evolution of the space-averaged Nusselt for different Rayleigh numbers and different dimensionless amplitudes. The monitoring points (1, 2, 3, 4) corresponding to the temporal position with the wall temperature (see fig.2).

Initially, all the curves illustrate transition from the conductive regime to an oscillatory behaviour. They show an exponential damping of the heat transfer. The duration of such transition growths with the increase of the Rayleigh number. After the transition time, the curves show a periodical evolution where the constant temperature formulation corresponds to the case of very low dimensionless amplitude (XA<<1).

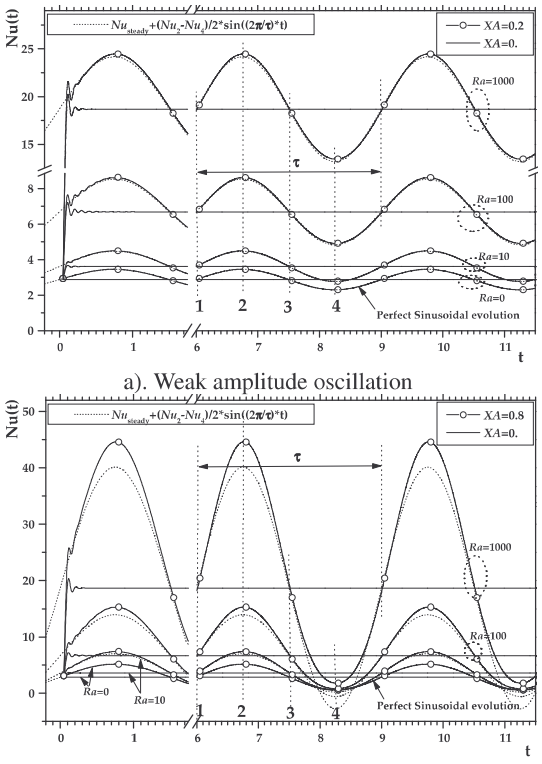

Figure 7 The space-average Nusselt number (Eqt 13)

In the conductive regime (Ra=0), the temporal evolution of the heat transfer is mainly sinusoidal for all the considered amplitudes, and the Nu evolution can be predicted as:

$$Nu = Nu_{\text{steady}} + \left(\left(Nu_2 - Nu_4\right)/2\right) \times \sin\left(\left(2\pi/\tau\right) \times t\right) \qquad (22)$$

where Nu_{steady} is the obtained steady state Nusselt number with constant temperature (XA=0). Nu_2 and Nu_4, are respectively the Nusselt numbers at the times 2 and 4.

The increase of Rayleigh number induces a loose of the symmetry time evolution in comparison to the constant wall temperature case, and this dissymmetry is more pronounced with the increase of the dimensionless amplitude (XA). In this case, Equation (22) is not valid. Note that the period is maintained at the temperature variation oscillation period (τ=3) for all the considered parameters.

Figure 8 demonstrates the effect of the dimensionless amplitude on the relative heat transfer enhancement ($\Delta Nu/Nu$), for different Rayleigh values. For low dimensionless amplitudes (XA<0.5), we observe an equivalence between constant and time dependent heating conditions (relative change is less than 5 %). For amplitudes greater than 0.5 we observe a significant heat transfer enhancement. This observed enhancement increases with the Ra number. For high Rayleigh number values, the heat transfer difference goes from the reference value to an increase of 19.5% when the dimensionless amplitude reaches 0.99.

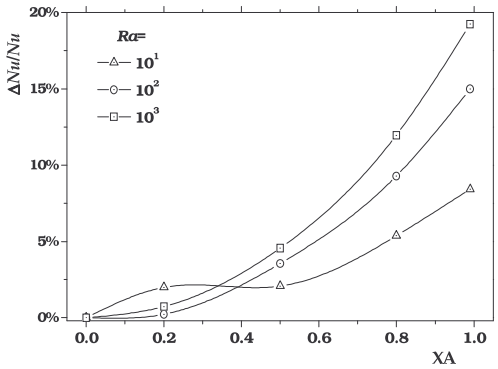

Figure 8 Influence of the temperature oscillation on the relative heat transfer enhancement

CONCLUSION

The problem of natural convection heat transfer in a vertical cylinder with open ends, filled with a fluid-saturated porous medium and heated with a sinusoidal lateral wall temperature, compared to a constant wall temperature, was the main focus of the present work. The dynamical results showed two types of flows, the mainly one directional and the flow with counter-flow.

The reverse flow (*Ra* and *Bi* dependent in the case of *A*=1) is a consequence of the pressure gradient effect occurring outside the thermal boundary layer.

The three principal domains of the *Bi* values (small, intermediate and high) are illustrated as follows:

- The weak and high Bi values, exhibit a constant asymptotic R_c tendency.
- The intermediate Bi values exhibit an increase of Ra_c with Bi connecting the two asymptotic values.

For the low dimensionless amplitudes case (*XA*<0.5), the obtained heat transfer in the sinusoidal time variation case is equivalent with the case of constant wall temperature where the difference is less than 5%. For high Rayleigh numbers, the equivalence in the heat transfer difference vanishes, the heat transfer difference goes from the reference value to an increase of 19.5% when the dimensionless amplitude reaches 0.99.

REFERENCES

[1] Patterson J.C., Imberger J., Unsteady natural convection in a rectangular cavity, *Int. J. Fluid Mech.* 100 (1980) 65-86.

[2] Vasseur P., Robillar L., Natural convection in a rectangular cavity with wall temperature decreasing at uniform misses, *Warme–und Stoffubertragung* 16 (1982) 199-207.

[3] Kazmierczak M., Chinoda Z., Boundary-driven flow in an enclosure with time periodic boundary conditions, *Int. J. Heat Mass Transfer* 35 (1992) 1507-1518.

[4] Sözen M. and Vafai K., Analysis of oscillating compressible flow through a packed bed, *Int. J. Heat Fluid Flow* 12 (1991) 130-136.

[5] Bradean R., Ingham D. B., Heggs P.J., and Pop I., Free convection fluid flow due to a periodically heated and cooled vertical plate embedded in a porous media, *Int. J. Heat Mass Transfer* 39 (1995) 2545-2557.

[6] Bradean R., Ingham D. B., Heggs P.J., and Pop I., Unsteady free convection adjacent to an impulsively heated horizontal circular in porous media, *Numer. Heat Transfer* A32 (1997) 325-346.

[7] Desrayaud G., Bennacer R., Caltagirone J. P., Chenier É., Joulin A., Laaroussi N., Mojtabi K., Étude numérique comparative des écoulements thermoconvectifs dans un canal vertical chauffé asymétriquement. *VIIIème Colloque Interuniversitaire Franco-Québécois*. 28-30 mai, Montréal, Canada, 2007.

[8] Krishnan A.S., Premachandran B., Balaji C., Venkateshan S.P., Combined experimental and numerical approaches to multi-mode heat transfer between vertical parallel plates, *Experimental Thermal and Fluid Science 29* (2004) 75–86.

[9] Hernandez J., Zamora B., Effects of variable properties and non-uniform heating on natural convection flows in vertical channels, *International Journal of Heat and Mass Transfer* 48 (2005) 793–807.

[10] Boland J.; The analytic solution of the differential equations describing heat flow in houses; *Building and environment* 37 (2002) 1027-1035.

[11]Patankar S. V., Numerical heat transfer fluid flux, *Hemisphere/McGraw-Hill*, New York, 1980.

[12] Bennacer R., El Ganaoui M., Leonardi E., Vertical Bridgman Configuration Heated From Below: 3D Bifurcation And Stability Analysis, *Applied Mathematical Modeling* 30 (11) (2006) 1249 1261.

[13] Ameziani, D. E., Bouhadef, K., Bennacer, R. and Rahli O., Analysis of the Chimney Natural Convection in a Vertical Porous Cylinder, *Numerical Heat Transfer, Part A: Applications*, 54:1,47-66 (2008)